RSC Advances

PAPER

View Article Online
View Journal | View Issue

Cite this: *RSC Adv.*, 2014, **4**, 27625

Gold nanoparticle-decorated MoS_2 nanosheets for simultaneous detection of ascorbic acid, dopamine and uric acid†

Haofan Sun,‡[a] Jie Chao,‡[b] Xiaolei Zuo,[b] Shao Su,*[a] Xingfen Liu,[a] Lihui Yuwen,[a] Chunhai Fan[ab] and Lianhui Wang*[a]

Received 3rd May 2014
Accepted 13th June 2014

DOI: 10.1039/c4ra04046e

www.rsc.org/advances

An electrochemical sensor has been developed for simultaneous detection of dopamine (DA), uric acid (UA) and ascorbic acid (AA) based on a gold nanoparticle-decorated MoS_2 nanocomposite (AuNPs@MoS_2) modified electrode. The AuNPs@MoS_2 nanocomposite has been synthesized by electrodeposition of AuNPs on the MoS_2 nanosheets, which possesses better properties than pure AuNPs and MoS_2. The AuNPs@MoS_2 film modified electrode showed excellent electrocatalytic activity toward the oxidation of AA, DA and UA with three well-resolved oxidation peaks. The peak separation of AA–DA, DA–UA and AA–UA is 151 mV, 137 mV and 288 mV, respectively, which permits the modified electrode to individually or simultaneously analyze AA, DA and UA by differential pulse voltammetry (DPV). Under optimum conditions, the AuNPs@MoS_2 modified electrode exhibits linear response toward AA, DA and UA in the range of 50–100 000 μM, 0.05–30 μM and 50–40 000 μM, respectively. Moreover, the MoS_2-based modified electrode was successfully employed to determine DA in human serum samples with satisfactory results.

1. Introduction

As we known, ascorbic acid (AA), dopamine (DA) and uric acid (UA) always coexist in the extracellular fluids of the central nervous system and serum in mammals, which play very important roles in human metabolism. For example, abnormal DA expression leads to neurological disorders such as schizophrenia, Parkinson's disease and attention deficit hyperactivity disorder (ADHD).[1–3] Therefore, accurate, fast and simultaneous detection of DA, AA and UA is critically important in analytical and diagnostic applications. However, it is still a challenge of simultaneous determination of AA, DA and UA at conventional solid electrodes, ascribing to their overlapping oxidation potential. In order to improve the determination without cross-interferences, modified electrodes have been developed for the simultaneous detection of AA, DA and UA. Up to now, polymer films,[4–6] nobel metal nanoparticles,[7] nanowires,[8] nanotubes[9] and nanocomposites[10–12] have been employed to prepare modified electrodes to simultaneous detection of AA, DA and UA. Among these modified electrodes, nanocomposites-based modified electrodes have been attracted greatly attentions because of their better properties than single nanomaterials, such as larger surface area and higher catalytic activity.

Nanocomposites, because of their unique electronic, optical, and catalytic properties, combined with possibly synergistic effects and unique properties of individual nanostructures, have been extensively employed in electrochemical filed in the past few years.[13,14] For example, gold-based and graphene-based nanocomposites have been extensively applications in electrochemical catalysis, sensors, capacitors and lithium batteries.[15–19] Molybdenum disulfide (MoS_2) is a two-dimensional nanomaterial, which has been receiving great attentions due to its ultra-thin structure and unique physical and chemical properties. MoS_2 has been proved that it can be easily exfoliated to single-layer or few-layer sheets. Moreover, the single-layer or few-layer MoS_2 nanosheets could be considered as a semiconducting analogous of graphene, which can be easily decorated with noble metal nanoparticles (such as gold, silver, palladium, platinum) and other nanostructures.[20,21] Such MoS_2-based nanocomposites have been expected to offer superior properties, which have been employed in many fields. Chen *et al.* synthesized ultrasmall Fe_3O_4 nanoparticles-decorated MoS_2 nanosheets and successfully used the MoS_2-based nanocomposites in lithium ion batteries with superior performances.[22] Huang's group had reported that AuNPs@MoS_2 can significantly enhance

[a]*Key Laboratory for Organic Electronics & Information Displays (KLOEID), Institute of Advanced Materials (IAM), School of Materials Science and Engineering, Nanjing University of Posts & Telecommunications, 9 Wenyuan Road, Nanjing, 210046, China. E-mail: iamssu@njupt.edu.cn; iamlhwang@njupt.edu.cn; Tel: +86 25 85866333*

[b]*Division of Physical Biology, Shanghai Institute of Applied Physics, Chinese Academy of Sciences, Shanghai 201800, China*

† Electronic supplementary information (ESI) available: The EDX of MoS_2 and AuNPs@MoS_2 nanocomposite (Fig. S1), effect of scan rate (Fig. S2) and pH on the peak current of AA, DA and UA (Fig. S3 and S4). See DOI: 10.1039/c4ra04046e

‡ These authors contributed equally to this work.

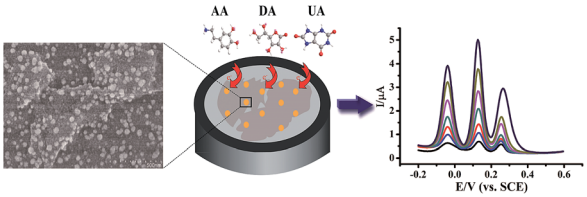

Scheme 1 Schematic illustrates of MoS_2-based electrochemical sensors.

electrocatalytic performance toward hydrogen evolution reactions.[23] Our group also had already employed AuNPs-decorated MoS_2 to construct electrochemical sensors for DA and glucose detections.[24,25]

In this work, the AuNPs@MoS_2 nanocomposite was prepared by electrochemical deposition method. The prepared nanocomposite possessed advantages of both AuNPs and MoS_2, resulting in excellent electrocatalytic activity for oxidation reactions of AA, DA and UA. As shown in Scheme 1, the peak potential separations were large enough to individually or simultaneously determine AA, DA and UA. In addition, the MoS_2-based modified electrode exhibited good sensitivity and selectivity for the determination of DA in human serum.

2. Experimental

2.1. Reagents and materials

Potassium hexacyanoferrate(III) ($K_3Fe(CN)_6$, ≥99.5%), Na_2HPO_4 and NaH_2PO_4 were purchased from Sinopharm Chemical Reagent Co., Ltd. Phosphate buffer (PB, 0.1 M, pH 6.0–8.0) solution was prepared from stock solutions of Na_2HPO_4 and NaH_2PO_4. Dopamine (DA), ascorbic acid (AA), uric acid (UA), gold(III) tetrachloride trihydrate ($HAuCl_4 \cdot 3H_2O$, ≥99%) and molybdenum(IV) sulfide powder (<2 mm, 99%), were purchased from Sigma-Aldrich. Aqueous solutions were prepared with ultrapure water from Millipore system (>18 MΩ cm). All chemicals were directly used without further purification.

2.2. Apparatus and measurements

Cyclic voltammetry (CV), different pulse voltammetry (DPV), and normal pulse voltammetry (NPV) were obtained by an Autolab PGSTAT302 (Metrohm China Ltd, Switzerland). The electrochemical experiments were tested by a conventional three-electrode system, in which a Pt wire and a saturated calomel electrode (SCE) were employed as the counter and the reference electrode, respectively. Different modified glass carbon electrodes (GCE) were employed as work electrodes. PB solution of 0.1 M (pH 7.0) was used as supporting electrolyte unless specifically illustration. Nitrogen bubbling is needed to restrain oxygenation in electrolyte solutions for at least 30 min and the electrochemical measurements were carried out under a nitrogen atmosphere. The morphology of nanocomposites was observed using a scanning electron microscope (SEM, S-4800, Hitachi).

2.3. Preparation of MoS_2

We employed the same method to fabricate few layer MoS_2 nanosheets as we previously reported.[25] Briefly, we prepared MoS_2 nanosheets by the intercalation exfoliation method developed by Joensen with some decorations.[26] 10 mL *n*-butyllithium solution was applied to form intercalted MoS_2 within Ar atmosphere at room temperature for about two days. The redundant *n*-butyllithium solution was removed and the residual solvent was removed by Ar gas flow. The exfoliation of Li intercalated MoS_2 was realized by adding deoxidation water and sonicating with the suspension for 1 hour. Finally, the aqueous dispersed MoS_2 nanosheets were centrifuged at least twice to remove the LiOH and other soluble impurities.

2.4. Preparation of AuNPs@MoS_2 nanocomposite decorated electrode

The GCE of 3 mm in diameter was polished mechanically with 0.3 μm and 0.05 μm-alumina powders and rinsed with ultrapure water between each polishing step. After this, it was sonicated with absolute ethanol and ultrapure water for about 1 min, respectively. 5 microliters of the MoS_2 solution were dropped to the surface of the GCE and allowed to dry in the ambient air for about 16 h, which denotes as MoS_2/GCE. The MoS_2/GCE was then immersed in 0.5 mM $HAuCl_4$ solution to form the AuNPs@MoS_2/GCE. The electrodeposition method: pulse voltammetry (1.1 V to −0.2 V), scan rate: 10 mV s^{-1}. For comparison, the AuNPs/GCE was prepared under the same condition.

3. Results and discussion

The morphologies of MoS_2 and AuNPs-decorated MoS_2 were observed by SEM. As shown in Fig. 1A, the exfoliated MoS_2 nanosheets displayed few and thin layers. With the electrodeposition of $HAuCl_4$, the AuNPs dispersed homogeneously onto the surface of MoS_2 nanosheets and the average diameter of AuNP was 50 nm. The SEM image indicates AuNPs@MoS_2 nanocomposite has successfully synthesized (Fig. 1B). The energy-dispersive X-ray spectroscopy (EDX) was also employed to confirm the presence of gold in the nanocomposite (Fig. S1†).

The electrochemical performances of AA, DA and UA on the different electrodes were investigated by cyclic voltammetry (CV). As shown in Fig. 2, a broad peak was obtained at 0.277 V by GCE (curve a), indicating that the bare GCE can't distinguish the AA, DA and UA. Unfortunately, both AuNPs/GCE (curve b) and MoS_2/GCE (curve c) also didn't simultaneously determine DA,

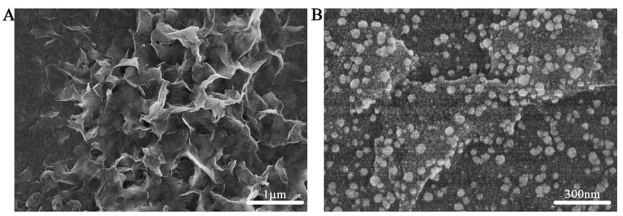

Fig. 1 SEM images of the (A) MoS_2 and (B) AuNPs@MoS_2 nanostructures at ITO.

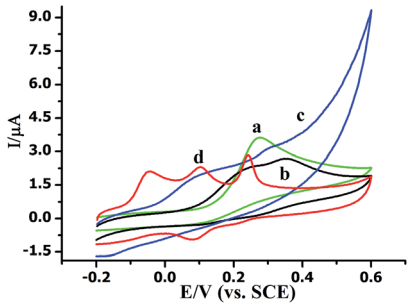

Fig. 2 Cyclic voltammograms of (a) bare GCE and (b) AuNPs/GCE (c) MoS_2/GCE (d) AuNPs@MoS_2/GCE in 0.1 M PB solution (pH 7.0) containing of 20 mM AA, 1 μM DA and 10 mM UA. Scan rate: 100 mV s^{-1}.

AA and UA. Only two oxidation peaks were observed at 0.241 V and 0.355 V at AuNPs/GCE and at 0.94 V and 0.317 V at MoS_2/GCE, respectively. However, three well-resolved oxidation peaks were observed at −0.046 V, 0.105 V and 0.242 V at AuNPs@MoS_2/GCE, indicated that the MoS_2-based modified electrode possessed excellent electrocatalytic oxidation toward AA, DA and UA (curve d). More importantly, the peak potential separation of AA–DA, DA–UA and AA–UA was 151 mV, 137 mV and 288 mV, respectively, which large enough to individual and simultaneous detection of AA, DA and UA. All the results suggested that the AuNPs@MoS_2/GCE possesses excellent electrochemical performance, which can simultaneously detect DA, AA and UA using electrochemical method.

The influence of scan rate and pH value on the electrochemical response of AuNPs@MoS_2/GCE toward AA, DA and UA was studied. As shown in Fig. 3A, the oxidation peak current of AA, DA and UA was linearly to the scan rate in the range of 10–300 mV s^{-1} indicating that the oxidation reaction was controlled by adsorption process. The cyclic voltammograms of AA, DA and UA at the AuNPs@MoS_2/GCE at different scan rate were displayed in Fig. S2.† The effect of pH on the catalytic response of AA, DA and UA at the AuNPs@MoS_2/GCE was also investigated over the pH range from 6.0 to 8.0. The results showed that the anodic peak potential of AA, DA and UA shifted to negatively with pH value increasing (Fig. 3B). Moreover, the oxidation peak potential of AA, DA and UA were linearly proportional to the pH value with a slope of −62.7, −51.8 and −57.1 mV per pH, respectively, suggesting protons were involved in electrochemical process (the DPV data displayed in Fig. S3†). The peak current of AA, DA and UA was also changed with the pH value increased (Fig. S4†). In this work, pH 7.0 was taken in our following investigation.

Individually or simultaneously determination AA, DA and UA at AuNPs@MoS_2/GCE was carried out by differential pulse voltammetric (DPV) technique. In ternary mixture, the concentration of only one species changed, while other species kept constant for selective detection at AuNPs@MoS_2/GCE. As shown in Fig. 4A, the electrochemical responses of AA linearly with the increasing AA concentration in range from 0.05 to 100 mM with detection limit of 50 μM. More important, the changes of AA

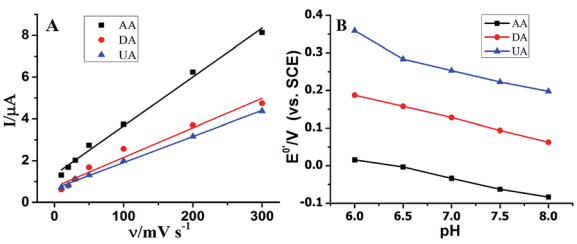

Fig. 3 (A) Effect of scan rate on the current and (B) effect of pH on the peak potential at AuNPs@MoS_2/GCE.

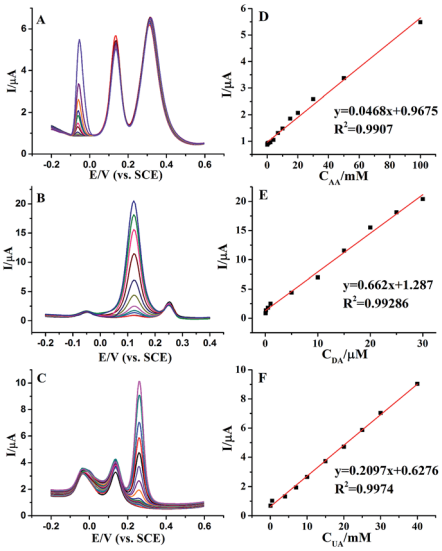

Fig. 4 DPV profiles at AuNPs@MoS_2/GCE in 0.1 M PB solution (pH 7.0) (A) containing 6 μM DA, 30 mM UA and different concentrations of AA from 0.05 mM to 100 mM, (B) containing 12 mM AA, 10 mM UA and different concentrations of DA from 0.05 μM to 30 μM, and (C) containing 50 mM AA, 4 μM DA and different concentrations of UA from 0.05 mM to 50 mM. (D–F) The plots of the oxidative peak currents *versus* the concentrations of AA, DA and UA.

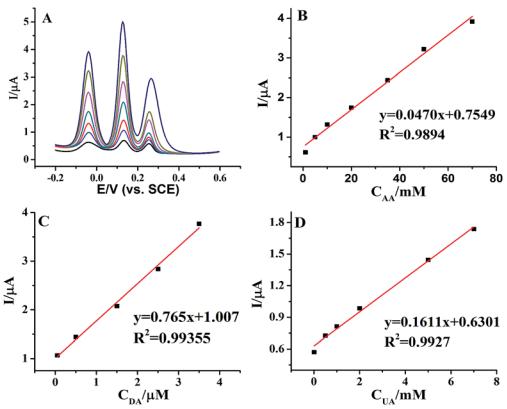

Fig. 5 (A) DPV profiles at AuNPs@MoS_2/GCE in 0.1 M PB solution (pH 7.0) containing different concentrations of AA, DA and UA. From bottom to up the concentrations from 1 mM to 70 mM for AA, 0.01 μM to 7 μM for DA and 0.01 mM to 12 mM for UA, respectively. (B–D) The plots of the oxidative peak currents *versus* the concentrations of AA, DA and UA.

Table 1 Comparison of the response characteristics of different modified electrodes for simultaneous detection of AA, DA and UA

	Detection limit (μM)			Liner range (μM)			
Electrode materials	AA	DA	UA	AA	DA	UA	Ref.
OMC/Nafion[a]	20	0.5	4.0	40–800	1–90	5–80	27
Nitrogen doped graphene	2.2	0.25	0.045	5–1300	0.5–170	0.1–200	28
Poly(Evans blue)/GCE	—	0.25	2	—	1.0–10	30–110	29
CILE[b]	20	1.0	1.0	50–7400	2.0–1500	2.0–2200	30
Poly(eriochrome black T)/GCE	10	0.02	1.0	150–1000	0.1–200	10–130	31
Pt–Au hybrid	103	24	21	103–165	24–384	21–336	32
Chitosan–graphene	50	1	2	50–1200	1–24	2–45	33
AuNPs–β-CD–Gra/GCE[c]	10	0.15	0.12	30–2000	0.5–150	0.5–60	34
AuNPs@MoS_2/GCE	100	0.05	10	10^3–7×10^4	0.05–4×10^3	10–7×10^3	This work

[a] Ordered mesoporous carbon/Nafion composite film. [b] Carbon ionic liquid electrode. [c] Gold nanoparticles–β-cyclodextrin–graphene.

concentration have no significant influence on the electrochemical performances of other two compounds. Similarly, the oxidation peak currents of DA (Fig. 4B) or UA (Fig. 4C) increased linear with the increasing concentration in the range from 0.05 to 30 μM and 0.05 to 40 mM with detection limit of 50 nM and 50 μM, respectively ($S/N = 3$). These results proved that the proposed MoS_2-based electrode can well separate and determine the DA, AA and UA when they co-exist in buffer solution.

Furthermore, we proved the feasibility of simultaneous determination of AA, DA and UA based on AuNPs@MoS_2/GCE. As shown in Fig. 5, the electrochemical response of AA, DA and UA still increases linear with the increase of their concentrations. The peak currents of AA, DA and UA were linear with the concentrations in the ranges from 1 mM to 70 mM, 50 nM to 4 mM and 10 μM to 7 mM with detection limit of 100 μM, 50 nM and 10 μM, respectively ($S/N = 3$). The present results are compared to other nanomaterials-based electrodes in Table 1, indicating that the analytical parameters including linear range and detection limit using AuNPs@MoS_2/GCE are better or comparable to the reported results at different modified electrodes. All the experimental results indicated that AuNPs@MoS_2 nanocomposite provides a comfortable condition which is suitable to individual or simultaneous determination of AA, DA and UA with high sensitivity and selectivity. Thus, AuNPs@MoS_2 nanocomposite with well electrocatalytic property is a promising material for constructing sensitive and selective biosensors and biofuel cells.

In order to verify the reliability of the method for detection in real samples, we took DA determination as an example in 1% human serum. The analysis of DA was investigated by the standard addition method and the results are shown in Table 2.

Table 2 Determination and recovery test of DA in human serum samples ($n = 4$)

DA specified (μM)	Added (μM)	Found (μM)	Recovery (%)	RSD (%)
1	0	1.013	101.30	2.64
1	9	9.823	98.03	2.99
1	14	15.291	102.08	2.66
1	24	25.246	101.03	2.71

The recovery and the relative standard deviation (RSD) were accurate and precise, indicating that successful applicability of the proposed electrode to determination of DA in the real biological samples.

4. Conclusion

An ultrasensitive biosensor for the determination of AA, DA and UA was fabricated by AuNPs@MoS_2 nanocomposite film modified electrode. The AuNPs@MoS_2/GCE exhibits excellent electrocatalytic oxidation towards AA, DA and UA, which can individually and simultaneously determine AA, DA and UA. It is a very simple method for preparation of MoS_2-based electrochemical sensor and can be very useful for detection of AA, DA and UA in buffer or in real sample. The AuNPs@MoS_2 nanocomposite may be a hopeful candidate nanomaterial for the development of electrochemical sensors for chemical and biological molecules determinations.

Acknowledgements

This work was financially supported by the National Basic Research Program of China (2012CB933301), the National Natural Science Foundation of China (21305070, 21204038, 81273409, 21375139), the Natural Science Foundation of Jiangsu Province (BK20130861), the Ministry of Education of China (IRT1148, 20123223110007, 20133223120013), the Priority Academic Program Development of Jiangsu Higher Education Institutions (PAPD), the Scientific Research Foundation of Nanjing University of Posts and Telecommunications (NY212033), Ordinary University Graduate Student Scientific Research Innovation Projects of Jiangsu Province (CXLX13_447).

Notes and references

1 A. Carlsson, *Psychol. Med.*, 1977, 7, 583–597.
2 R. M. Wightman, L. J. May and A. C. Michael, *Anal. Chem.*, 1988, **60**, 769A–793A.
3 G. LaHoste, J. Swanson, S. Wigal, C. Glabe, T. Wigal, N. King and J. L. Kennedy, *J. Mol. Psychiatr.*, 1996, **1**, 121–124.

4 L. M. Niu, K. Q. Lian, H. M. Shi, Y. B. Wu, W. J. Kang and S. Y. Bi, *Sens. Actuators, B*, 2012, **178**, 10–18.
5 Y. Wang and C. Bi, *J. Mol. Liq.*, 2012, **177**, 26–31.
6 X. Zheng, X. Zhou, X. Ji, R. Lin and W. Lin, *Sens. Actuators, B*, 2013, **178**, 359–365.
7 M. S. Hsu, Y. L. Chen, C. Y. Lee and H. T. Chiu, *ACS Appl. Mater. Interfaces*, 2012, **4**, 5570–5575.
8 S. Su, X. Wei, Y. Guo, Y. Zhong, Y. Su, Q. Huang, C. Fan and Y. He, *Part. Part. Syst. Charact.*, 2013, **30**, 326–331.
9 J. Zhao, W. Zhang, P. Sherrell, J. M. Razal, X. F. Huang, A. I. Minett and J. Chen, *ACS Appl. Mater. Interfaces*, 2011, **4**, 44–48.
10 J. Zhou, M. Chen and G. Diao, *ACS Appl. Mater. Interfaces*, 2013, **5**, 828–836.
11 C. Liu, K. Wang, S. Luo, Y. Tang and L. Chen, *Small*, 2011, **7**, 1203–1206.
12 F. Xiao, J. Song, H. Gao, X. Zan, R. Xu and H. Duan, *ACS Nano*, 2011, **6**, 100–110.
13 A. Yu, Z. Liang, J. Cho and F. Caruso, *Nano Lett.*, 2003, **3**, 1203–1207.
14 S. Hrapovic, Y. Liu, K. B. Male and J. H. Luong, *Anal. Chem.*, 2004, **76**, 1083–1088.
15 Y. J. Kang, J. W. Oh, Y. R. Kim, J. S. Kim and H. Kim, *Chem. Commun.*, 2010, **46**, 5665–5667.
16 G. Yu, L. Hu, M. Vosgueritchian, H. Wang, X. Xie, J. R. McDonough, X. Cui, Y. Cui and Z. Bao, *Nano Lett.*, 2011, **11**, 2905–2911.
17 E. Yoo, J. Kim, E. Hosono, H. S. Zhou, T. Kudo and I. Honma, *Nano Lett.*, 2008, **8**, 2277–2282.
18 H. Wang, Y. Yang, Y. Liang, J. T. Robinson, Y. Li, A. Jackson, Y. Cui and H. Dai, *Nano Lett.*, 2011, **11**, 2644–2647.
19 J. Liang, Z. Chen, L. Guo and L. Li, *Chem. Commun.*, 2011, **47**, 5476–5478.
20 L. Yuwen, F. Xu, B. Xue, Z. Luo, Q. Zhang, B. Bao, S. Su, L. Weng, W. Huang and L. H. Wang, *Nanoscale*, 2014, **6**, 5762–5769.
21 X. Huang, Z. Zeng, S. Bao, M. Wang, X. Qi, Z. Fan and H. Zhang, *Nat. Commun.*, 2013, **4**, 1444.
22 Y. Chen, B. Song, X. Tang, L. Lu and J. Xue, *Small*, 2014, **10**, 1536–1543.
23 J. Kim, S. Byun, A. J. Smith, J. Yu and J. Huang, *J. Phys. Chem. Lett.*, 2013, **4**, 1227–1232.
24 S. Su, H. Sun, F. Xu, L. Yuwen, C. Fan and L. Wang, *Microchim. Acta*, 2014, DOI: 10.1007/s00604-014-1178-9.
25 S. Su, H. Sun, F. Xu, L. Yuwen and L. Wang, *Electroanalysis*, 2013, **25**, 2523–2529.
26 P. Joensen, R. Frindt and S. R. Morrison, *Mater. Res. Bull.*, 1986, **21**, 457–461.
27 D. Zheng, J. Ye, L. Zhou, Y. Zhang and C. Yu, *J. Electroanal. Chem.*, 2009, **625**, 82–87.
28 Z. H. Sheng, X. Q. Zheng, J. Y. Xu, W. J. Bao, F. B. Wang and X. H. Xia, *Biosens. Bioelectron.*, 2012, **34**, 125–131.
29 L. Lin, J. Chen, H. Yao, Y. Chen, Y. Zheng and X. Lin, *Bioelectrochemistry*, 2008, **73**, 11–17.
30 A. Safavi, N. Maleki, O. Moradlou and F. Tajabadi, *Anal. Biochem.*, 2006, **359**, 224–229.
31 C. F. Tang, S. A. Kumar and S. M. Chen, *Anal. Biochem.*, 2008, **380**, 174–183.
32 S. Thiagarajan and S. M. Chen, *Talanta*, 2007, **74**, 212–222.
33 D. Han, T. Han, C. Shan, A. Ivaska and L. Niu, *Electroanalysis*, 2010, **22**, 2001–2008.
34 X. Tian, C. Cheng, H. Yuan, J. Du, D. Xiao, S. Xie and M. M. Choi, *Talanta*, 2012, **93**, 79–85.